
SUSTOX - A Numerical Simulator for Fluid and Species Transport in the Subsurface



RODOS
REPORT

DECISION SUPPORT FOR NUCLEAR EMERGENCIES

SUSTOX - A Numerical Simulator for Fluid and Species Transport in the Subsurface

RODOS(WG4)-TN(99)06

S.L.Kivva

Institute of Mathematical Machines & Systems Problems (IPMMS)
pr.Glushkova, 42,
252207 Kiev,Ukraine
Email: slk@dem.ipmms.kiev.ua

December 5, 1997

Summary

This report contains a technical description of the SUSTOX computer program for simulating the fluid and species transport in variably saturated porous media. The physical processes taken into account in SUSTOX are discussed, and the governing equations solved by the simulator are stated in full detail. A brief overview is given of the mathematical and numerical methods. The report provides description of SUSTOX input file. Code applications are illustrated by means of two sample problems.

Contents

SUMMARY	1
CONTENTS	2
1 INTRODUCTION	3
2 GOVERNING EQUATIONS	4
2.1 <i>Water Flow Equation</i>	4
2.2 <i>Species Transport Equation</i>	6
3 NUMERICAL APPROXIMATION	9
3.1 <i>Water flow equation</i>	9
3.2 <i>Species Transport Equation</i>	11
3.3 <i>Boundary Condition Approximation</i>	12
4 NUMERICAL SOLUTION METHOD	13
5 COMPARISONS WITH EXISTING SOLUTIONS	15
5.1 <i>Philip's Vertical Infiltration Problem</i>	15
5.2 <i>Unsaturated Species Transport</i>	16
6 RADIONUCLIDES MIGRATION IN THE SUBSURFACE AROUND THE CHERNOBYL NPP	18
6.1 <i>Site Description</i>	18
6.2 <i>Simulation Results</i>	19
7 INPUT FILE STRUCTURE	25
7.1 <i>Simulation Title Card</i>	25
7.2 <i>Solution Schemes Card</i>	25
7.3 <i>Numerical Control Card</i>	25
7.4 <i>Grid Geometry Card</i>	26
7.5 <i>Inactive Nodes Card</i>	27
7.6 <i>Rock or Soil Types Card</i>	27
7.7 <i>Mechanical Properties Card</i>	27
7.8 <i>Hydraulic Properties Card</i>	28
7.9 <i>Species Properties Card</i>	28
7.10 <i>Soil Characteristics Card</i>	29
7.11 <i>Liquid Relative Permeability Card</i>	30
7.12 <i>Liquid Boundary Conditions Card</i>	32
7.13 <i>Species Boundary Conditions Card</i>	34
7.14 <i>Fuel Particle Sources Card</i>	36
7.15 <i>Initial Conditions Card</i>	36
7.16 <i>Sources and Sinks Card</i>	37
7.17 <i>Output Control Card</i>	40
8 REFERENCES	42
APPENDIX	44
A. <i>Input File of Philip's Infiltration Problem</i>	44
B. <i>Input File of Unsaturated Species Transport Problem</i>	47
DOCUMENT HISTORY	53

1 Introduction

SUSTOX code is developed to simulate liquid flow and transport of radionuclides, heavy metals, or other contaminants in variably saturated subsurface environment. The description of porous media contamination is founded on governing conservation equations and associated constitutive functions. Liquid flow through the subsurface environment occurs in response to gradients in liquid pressures and gravitational body forces according to Darcy's flow law. Species transport through the variably saturated porous media occurs by molecular diffusion, hydrodynamic dispersion, and advection. Interphase species mass transfer between exchangeable sorbed solid aqueous phases is assumed being under thermodynamic and geo-chemical equilibrium conditions. These equilibrium condition assumptions require that time scales for thermodynamic and geo-chemical phenomena be small when compared with those for transport phenomena. Slow sorption/desorption processes between exchangeable sorbed solid and fixed solid phases are considered as non-equilibrium exchangeable processes which are described by first-order kinetic equations.

Governing equations are partial differential equations for the conservation of liquid mass and species mass. The governing partial differential equations are solved by discretizing governing equations to algebraic form with integrated finite-difference method. The resulting system of algebraic equations is non-linear. The non-linear algebraic forms of the conservation equations are converted to a linear form using residual-based, global Newton's iteration technique. The technique generally yields quadratic convergence of the residuals with iterations, given initial estimates of the unknowns that are sufficiently close to the solution. Conjugate gradient scheme is used for the solution of the linearized algebraic form of the conservation equations.

2 Governing Equations

2.1 Water Flow Equation

The mathematical description of the water transport in the variably saturated subsurface implies assumptions which are commonly done for this type of problems. It is assumed that fluid transport through soil occurs in response to pressure gradients and gravitational body forces followed Darcy's flow equations. The porous medium is considered to be rigid. Pressure gradients in the gas phase to be negligible so that gas pressure remains effectively constant at atmospheric pressure.

Neglecting hysteresis and temperature gradients, movement of moisture through a saturated-unsaturated porous medium is described by

$$\frac{\partial}{\partial t}(\phi S \rho) = \frac{\partial}{\partial x_i} \left[\frac{\rho k_r k_{ij}}{\mu} \left(\frac{\partial p}{\partial x_j} + \rho g \frac{\partial z}{\partial x_j} \right) \right] + f \quad (1)$$

where t is the time (T); x_i are the cartesian spatial coordinates (L); ϕ is the porosity of the medium; ρ is the fluid density (ML^{-3}); k_{ij} are components of the intrinsic permeability tensor (L^2); k_r is the relative permeability ($0 \leq k_r \leq 1$); μ is the fluid dynamic viscosity ($ML^{-1}T^{-1}$); p is the fluid pressure ($ML^{-1}T^{-2}$); g is the gravitational constant (LT^{-2}); z is the elevation measured from a reference datum (L); f represents sources or sinks of fluid in the system ($ML^{-3}T^{-1}$); and S is the volumetric saturation.

The soil water retention curve is calculated as a function of tension head ψ by using the following expressions:

- van Genuchten model [1]

$$\frac{S - S_r}{1 - S_r} = \left[1 + (\alpha \psi)^n \right]^{-m} \quad \psi > 0 \quad (2)$$

$$S = 1 \quad \psi \leq 0$$

where S_r is the residual saturation; and α (L^{-1}) and n are empirical parameters determined experimentally; m is given by

$$m = 1 - (1/n)$$

- Brooks and Corey model [2]

$$\frac{S - S_r}{1 - S_r} = \left(\frac{\psi}{\psi^*} \right)^{-m} \quad \psi < \psi^* \quad (3)$$

$$S = 1 \quad \psi \geq \psi^*$$

where ψ^* is the minimum drainage capillary pressure at which a continuous non-wetting phase exists; m is a empirical parameter related to the pore-size distribution of the porous medium.

- Haverkamp 1 model [3]

$$\frac{S - S_r}{1 - S_r} = \frac{\alpha}{\alpha + |\psi|^\beta} \quad \psi > 0 \quad (4)$$

$$S = 1 \quad \psi \leq 0$$

where α and β are curve-fitting parameters.

- Haverkamp 2 model [3]

$$\frac{S - S_r}{1 - S_r} = \frac{\alpha}{\alpha + (\ln|\psi|)^\beta} \quad \psi > 0 \quad (5)$$

$$S = 1 \quad \psi \leq 0$$

where α and β are curve-fitting parameters.

The formulas (2)-(5) can be combined with the predictive conductivity models of Mualem [4] and Burdine [5] to yield an expression for relative permeability $k_r(S)$ of the forms:

- van Genuchten with Mualem model

$$k_r = \sqrt{S^*} \left[1 - \left(1 - S^{*1/m} \right)^m \right]^2$$

where S^* is the effective saturation defined by

$$S^* = \frac{S - S_r}{1 - S_r}$$

- van Genuchten with Burdine model

$$k_r = S^{*2} \left[1 - \left(1 - S^{*1/m} \right)^m \right]^{1/2}$$

- Brooks and Corey with Mualem model

$$k_r = S^{*(5/2+2/m)}$$

- Brooks and Corey with Burdine model

$$k_r = S^{*(3+2/m)}$$

- Haverkamp model [3]

$$k_r = \frac{A}{A + |\psi|^B}$$

where A and B are curve-fitting parameters.

- Touma and Vauclin model [6]

$$k_r = A(S\phi)^B$$

where A and B are empirical fitting parameters.

The initial conditions for equation (1) consist of initial values of pressure, specified by:

$$p(x,0) = \varphi(x),$$

where x is the spatial coordinate vector and φ is a prescribed function.

Boundary conditions may be Dirichlet (type 1):

$$p(x,t) = g_1(x,t) \quad \text{on } \Gamma_1,$$

or Neumann (type 2):

$$\left[k_r \frac{k_{ij}}{\mu} \left(\frac{\partial p}{\partial x_j} + \rho g \frac{\partial z}{\partial x_j} \right) \right] n_i = g_2(x,t) \quad \text{on } \Gamma_2,$$

where g_1 is the prescribed pressure on the boundary Γ_1 ; n_i is the i th component of the unit vector normal to the boundary Γ_2 , direction outward; and g_2 is the prescribed outward fluid flux normal to Γ_2 . Γ_1 and Γ_2 comprise the entire boundary of the domain. Usually Γ_1 is the part of boundary at which surface-water bodies are intercepted by aquifers; Γ_2 are the boundaries across which fluid passes at a specific rate (impervious boundaries, areas of infiltration or evapotranspiration, points of injection and withdrawal, etc.).

2.2 Species Transport Equation

Let c_l represent the volumetric radionuclide activity in the aqueous phase (ML^{-3}); c_s the volumetric exchangeable sorbed activity in solid phase (ML^{-3}); and c_f the volumetric activity which is fixed in the mineral lattice (ML^{-3}). Assuming that the ion-exchange reaction transferring activity between aqueous and solid exchangeable phases has a sufficiently short timescale, we will consider this reaction as instantaneous which is described by a linear equilibrium isotherm. Transfers of activity to and from the fixed phase are modelled by first-order rate constants α_{sf} and α_{fs} , respectively, as shown in Figure 1 [7].

The leaching of radionuclides from the fuel particles is modelled by a first-order equation

$$\frac{\partial c_p}{\partial t} = -(\alpha_p + \lambda)c_p, \quad (6)$$

$$c_p(0, x) = c_p^0(x),$$

where c_p is the radionuclide activity in the fuel particles per soil solid volume (ML^{-3}); α_p is the first-order constant of radionuclide leaching from fuel particles (T^{-1}); λ is the radionuclide decay constant (T^{-1}); c_p^0 is the initial radionuclide activity in the fuel particles (ML^{-3}).

Ignoring chemical diffusion in the solid phase, the equation for advective-dispersive transport of radionuclide activity in the exchangeable phase in variably saturated media may be written in the form

$$\frac{\partial c}{\partial t} = \frac{\partial}{\partial x_i} \left(\phi S D_{ij} \frac{\partial c_l}{\partial x_j} \right) - \frac{\partial}{\partial x_i} (v_i c_l) - \lambda c + (1 - n_T)(\alpha_p c_p + \alpha_{fs} c_f - \alpha_{sf} c_s) \quad (7)$$

where c is the radionuclide activity per total volume (ML^{-3}).

D_{ij} is the dispersion tensor, defined by:

$$\phi S D_{ij} = \alpha_T |v| \delta_{ij} + (\alpha_L - \alpha_T) \frac{v_i v_j}{|v|} + \phi S \tau D_0 \delta_{ij}$$

where α_L and α_T are the longitudinal and transverse dispersivities (L), respectively; δ_{ij} is the Kronecker delta; $|v|$ is the magnitude of the Darcy velocity; D_0 is the molecular diffusion coefficient ($L^2 T^{-1}$); and τ is the tortuosity.

The tortuosity may be computed from the Millington and Quirk [8] expression based on theoretical pore-size distribution models for partially saturated porous media

$$\tau = \phi^{10/3} S^{4/3}$$

The total radionuclide activity is defined by:

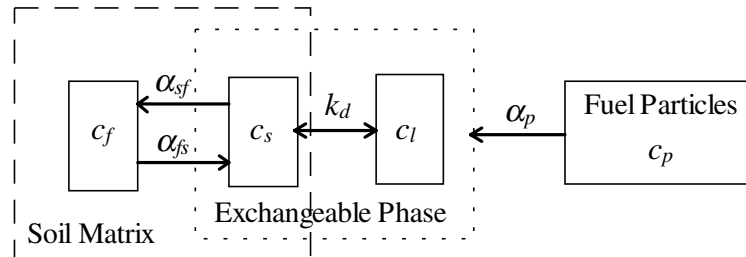


Figure 1. Schematic representation of the kinetic sorption model.

$$c = \phi S c_l + (I - \phi_T) c_s$$

where ϕ_T is the total porosity of the medium; and volumetric phase activities are interrelated through solid-aqueous partition coefficient k_d , according to relationship

$$k_d = \frac{c_s \rho}{c_l \rho_s}$$

where ρ_s is the soil solid density (ML^{-3}).

Initial conditions for equation (7) consist of specification of initial radionuclide activity in the aqueous phase:

$$c_l(x, t) = c_0(x)$$

Boundary conditions for inflow boundaries are Dirichlet (type 1):

$$c_l = c_I \quad \text{on } \Gamma_3$$

or Cauchy (type 3):

$$\left(-\phi S D_{ij} \frac{\partial c_l}{\partial x_j} + v_i c_l \right) n_i = v_b c_b \quad \text{on } \Gamma_4$$

where c_l is prescribed radionuclide activity on the boundaries Γ_3 ; n_i is the unit vector normal to boundaries, direction inwards; v_b is the prescribed fluid flux normal to the boundaries Γ_4 ; and c_b is the prescribed radionuclide activity associated with the prescribed fluid flux.

At outflow boundaries the assumption is often made that transport across the boundaries, according to Frind[9], occurs by advection only and a Neumann (type 2) boundary condition is specified by:

$$\frac{\partial c_l}{\partial x_j} = 0 \quad \text{on } \Gamma_5$$

where $\Gamma_3 + \Gamma_4 + \Gamma_5 = \Gamma$ is the boundary of the domain.

The transport of activity in the fixed phase is described by

$$\frac{\partial c_f}{\partial t} = \alpha_{sf} c_s - \alpha_{fs} c_f - \lambda c_f, \quad (8)$$

$$c_f(0, x) = c_f^0(x),$$

where c_f^0 is the initial activity in the fixed phase.

3 Numerical Approximation

The flow domain is spatially discretized into a computational domain composed of a number of non-overlapping control volumes. Each control volume surrounds a single grid point, which defines the position of intrinsic property variables. Surfaces between nodes are located at the midpoint between two adjacent nodes. Control volumes are defined by their bounding surfaces.

3.1 Water flow equation

The water mass conservation equation is discretized by integration the equation (1) over a control volume V and a short time interval τ .

$$\int_t^{t+\tau} \int_V \left[\frac{\partial}{\partial t} (\phi S \rho) - \frac{\partial}{\partial x_i} \left[\frac{\rho k_r k_{ij}}{\mu} \left(\frac{\partial p}{\partial x_j} + \rho g \frac{\partial z}{\partial x_j} \right) \right] - f \right] dV dt = \quad (9)$$

$$= \int_V (\phi S \rho) \Big|_t^{t+\tau} dV - \int_t^{t+\tau} \int_{\Gamma} \left[\frac{\rho k_r k_{ij}}{\mu} \left(\frac{\partial p}{\partial x_j} + \rho g \frac{\partial z}{\partial x_j} \right) \right] \cdot n d\Gamma dt - \int_t^{t+\tau} \int_V f dV dt = 0$$

where Γ is the boundary surface of the control volume V ; n is the unit vector normal to the boundary Γ .

Using fully implicit temporal discretization and approximating the surface integrals as summations over the bounding control volume surfaces, the equation (9) can be rewritten in form

$$V \frac{(\phi S \rho)^{t+\tau} - (\phi S \rho)^t}{\tau} - \sum_{\gamma} U_{\gamma}^{t+\tau} A_{\gamma} - V f^{t+\tau} = 0 \quad (10)$$

$$U_{\gamma} = - \frac{\rho k_r k_{ij}}{\mu} \left(\frac{\partial p}{\partial x_j} + \rho g \frac{\partial z}{\partial x_j} \right)$$

where A_{γ} is the area of control volume bounding surface γ ; U_{γ} is the water mass flux across the surface γ .

In order to define a value of U_{γ} at the surface γ located between two adjacent nodes $x_{j,p}$ and $x_{j,p-1}$, we integrate $\frac{\mu}{\rho k_r k_{ij}} U_{\gamma}$ over the interval $[x_{j,p-1}, x_{j,p}]$

$$- \int_{x_{j,p-1}}^{x_{j,p}} \frac{\mu U_{\gamma}}{\rho k_r k_{ij}} dx_j = \int_{x_{j,p-1}}^{x_{j,p}} \left(\frac{\partial p}{\partial x_j} + \rho g \frac{\partial z}{\partial x_j} \right) dx_j = (p + \rho g z) \Big|_{x_{j,p-1}}^{x_{j,p}}$$

Assuming constant U_γ between two adjacent nodes $x_{j,p}$ and $x_{j,p-1}$ yields

$$U_\gamma = -a_{j,p}(p + \rho g z)_{x_{j,p}}^- \quad (11)$$

where

$$a_{j,p} = \left[\int_{x_{j,p-1}}^{x_{j,p}} \frac{\mu}{\rho k_r k_{ij}} dx_j \right]^{-1}$$

$$y_{x_{j,p}}^- = \frac{y(x_{j,p}) - y(x_{j,p-1})}{x_{j,p} - x_{j,p-1}}$$

The coefficient $a_{j,p}$ can be computed by using following interface averages:

- harmonic weighting

$$a_{j,p} = \frac{2K_{p-1}K_p}{K_{p-1} + K_p}$$

- geometric weighting

$$a_{j,p} = \sqrt{K_{p-1}K_p}$$

- arithmetic weighting

$$a_{j,p} = 0.5(K_{p-1} + K_p)$$

where $K_p = \left(\frac{\rho k_r k_{ij}}{\mu} \right)$ at the point $x_{j,p}$.

Combining (10)-(11), the water mass conservation equation (1) is approximated by fully implicit finite-difference scheme

$$(\rho S \phi)_t^- - \left(a (p + \rho g z)_{x_j}^- \right)_{\hat{x}_i} - f = 0$$

where topped with bar subscript x_i represents the x_i -direction finite-difference left derivative and subscript x_i topped with circumflex represents the x_i -direction following finite-difference derivative

$$y_{\hat{x}_i} = \frac{y(x_{i,p+1}) - y(x_{i,p})}{0.5(x_{i,p+1} - x_{i,p-1})}$$

3.2 Species Transport Equation

Integration of the species transport equation (7) over a control volume V and a temporal interval $[t, t+\tau]$ and converting of the volumetric integrals into surface integrals yields

$$\begin{aligned} & \int_t^{t+\tau} \int_V \left[\frac{\partial c}{\partial t} - \frac{\partial}{\partial x_i} \left(\phi SD_{ij} \frac{\partial c_l}{\partial x_j} \right) + \frac{\partial}{\partial x_i} (v_i c_l) + \lambda c - (1 - n_T)(\alpha_p c_p + \alpha_{fs} c_f - \alpha_{sf} c_s) \right] dV dt = \\ & = \int_V [c(x, t + \tau) - c(x, t)] dV - \int_t^{t+\tau} \int_{\Gamma} \left[\phi SD_{ij} \frac{\partial c_l}{\partial x_j} - v_i c_l \right] \cdot n d\Gamma dt + \\ & + \int_t^{t+\tau} \int_V [\lambda c - (1 - n_T)(\alpha_p c_p + \alpha_{fs} c_f - \alpha_{sf} c_s)] dV dt = 0 \end{aligned}$$

Using fully implicit temporal discretization, applying the upstream-weighted approximation to advective flux term and approximating the surface integrals as summations over the control volume surface, we obtain the following monotone conservative implicit scheme

$$\begin{aligned} c_i^- - (b_{c\bar{x}_j})_{\hat{x}_i} + v_{i+0.5}^- c_{lx_i} + v_{i-0.5}^+ c_{\bar{l}x_i} + v_{i+0.5, \hat{x}_i} c_l - \\ - \lambda c + (1 - n_T)(\alpha_p c_p + \alpha_{fs} c_f - \alpha_{sf} c_s) = 0 \end{aligned}$$

where

$$b_{j,p} = \left[\int_{x_{j,p-1}}^{x_{j,p}} \frac{1}{\phi SD_{ij}} dx_j \right]^{-1}$$

$$y^\pm = 0.5(y \pm |y|)$$

$$y_{i\pm 0.5} = y(0.5(x_{i,p} + x_{i,p\pm 1}))$$

Integration the leaching equation (6) over a time interval leads to

$$c_p(t + \tau) = c_p(t) \exp\{-(\alpha_p + \lambda)\tau\}$$

Equation of radionuclide activity exchange between fixed and sorbed phases is discretized by integration the equation (8) over a small time interval

$$\begin{aligned}
& \int_t^{t+\tau} \left(\frac{\partial c_f}{\partial t} - \alpha_{sf} c_s + \alpha_{fs} c_f + \lambda c_f \right) dt = \\
& c_f \Big|_t^{t+\tau} - \int_t^{t+\tau} (\alpha_{sf} c_s - \alpha_{fs} c_f - \lambda c_f) dt = 0
\end{aligned} \tag{12}$$

Using fully implicit temporal approximation, we rewrite (12) in form

$$c_{f\bar{t}} - \alpha_{sf} c_s + \alpha_{fs} c_f + \lambda c_f = 0$$

3.3 *Boundary Condition Approximation*

The discretization of the water flow and species transport equations described above were obtained for nodes positioned within the interior of the computational domain. For nodes located adjacent to the domain boundary, the discretization of the governing equations differs to account for conditions at the boundary. Boundary conditions are specified either with field variables or with surface fluxes on the boundary surfaces. Boundary conditions of the former type are referred to as Dirichlet, whereas the latter type are referred to as Neumann.

Implementation of Dirichlet boundary conditions requires relatively few modifications to the discretized governing conservation equations. These modifications are replacing the following field variables at the boundary nodes by their values on the boundary surfaces.

Neumann-type boundary conditions are accommodated by substituting the specified surface fluxes directly into the discretized form of the conservation equation. Default boundary conditions for SUSTOX are zero-flux Neumann-type boundaries.

4 Numerical Solution Method

The finite difference discretization of the water flow equations leads to a system of non-linear equations:

$$F(x) = 0 \quad F: R^n \rightarrow R^n \quad (13)$$

The non-linear equations (13) are solved iteratively, using a multivariable, residual-based Newton technique

$$x^{s+1} = x^s + p_s \quad s = 0, 1, 2, \dots \quad (14)$$

$$p_s = -J(x^s)^{-1} F(x^s)$$

where s denotes an iteration number; and $J(x^s)$ is the Jacobian of $F(x)$.

It is well known that Newton iterations for a differentiable function $F(x)$ are quite powerful as soon as an initial guess x^0 is closely located to the solution x^* of the system (). In this case, the Newton method converges with quadratic rate. Unfortunately, it may converge slowly or does not converge at all if an initial guess is not good. In order to ensure global convergence, we replace the process (14) by following iterations

$$x^{s+1} = x^s + \lambda_s p_s$$

where λ satisfies to

$$f(x^s + \lambda_s p_s) \leq f(x^s) + \alpha \lambda_s \nabla f(x^s)^T p_s \quad \alpha \in (0, 1)$$

$$\nabla f(x^s + \lambda_s p_s)^T p_s \geq \beta \nabla f(x^s)^T p_s \quad \beta \in (\alpha, 1)$$

$$f(x) = \frac{1}{2} F(x)^T F(x) = \frac{1}{2} \|F(x)\|_2^2$$

Iteration continues until the criterion is satisfied

$$\max_{1 \leq i \leq n} \frac{|x_i^{s+1} - x_i^s|}{|x_i^s|} \leq \varepsilon$$

where ε is a user-provided error tolerance.

The iteration routine starts, at a given time step, with an estimate of liquid pressures based on the previous time step. This estimate is used to update values of the governing equation residuals and to evaluate all of the partial derivatives that make up the Jacobian matrix. The resulting system of linear equations is then solved by using the conjugate gradient method with incomplete LU factorization. Solution of the system of equations

yields changes to the liquid pressures. An iteration ends by updating the liquid pressures with the changes computed from the system of linear equations. If the criterion is satisfied, then the procedure is determined to have converged and a new time step begins. Otherwise, another iteration commences. If the criterion is not satisfied within a specified number of iterations, the system is considered non-convergent. Non-convergent systems are handled by reducing the simulation step, resetting the liquid pressures to their previous time-step values, and reinitiating the time-step procedures.

5 Comparisons with Existing Solutions

5.1 Philip's Vertical Infiltration Problem

Semi-analytic solution reported by Philip [11] for one-dimensional, time-dependent, unsaturated, vertical infiltration problem is used to demonstrate the SUSTOX possibility to correctly solve the one-dimensional Richard's equation for a wetting front in a semi-infinite porous media.

The problem domain is a column of 15-cm depth soil for which moisture-retention curve and liquid relative permeability are described by Haverkamp relations [3]:

$$\frac{S - S_r}{1 - S_r} = \frac{\alpha}{\alpha + (\ln|100\psi|)^\beta} \quad \psi < 0$$

$$S = 1 \quad \psi \geq 0$$

$$k_r = \frac{A}{A + (100\psi)^B}$$

where ψ is the tension head. The parameter values used in simulations are given in Table 1.

Table 1. Parameter values used in simulations.

Parameter	Value
saturated volumetric moisture content ϕ	0.495
residual volumetric moisture content S_r	0.124
curve-fitting parameter α	739
curve-fitting parameter β	4.0
saturated hydraulic conductivity K , cm/h	0.04428
curve-fitting parameter A	124.6
curve-fitting parameter B	1.77

The initial conditions for problem domain are specified as a uniform pressure head of -601.8 cm. A saturation boundary condition is assigned at the upper boundary, and constant pressure at the initial value is used at the lower boundary. Infiltration begins at time zero from the saturated upper boundary.

Table 2. Values of parameters used in simulations.

Item	Value
Diffusive porosity	0.45
Hydraulic conductivity, cm/day	1.0
Molecular diffusivity, cm ² /day	1.0
Tortuosity	1.0

Liquid pressure head at the end of 2.0 hours of infiltration is compared with the analytic results which were generated by the INFIL computer code [11]. Results of this comparison are shown in Figure 2. The SUSTOX input file for Philip's infiltration problem is given in appendix A.

5.2 Unsaturated Species Transport

Ross et al. [12] proposed to consider the transport in a one-dimensional, semi-infinite, horizontal tube of partially saturated soil as a test problem. The object of this problem is to determine the species concentration field in a tube of soil that has a uniform initial species concentration and moisture content and in which the upstream boundary is maintained at a prescribed moisture content and a prescribed solute concentration.

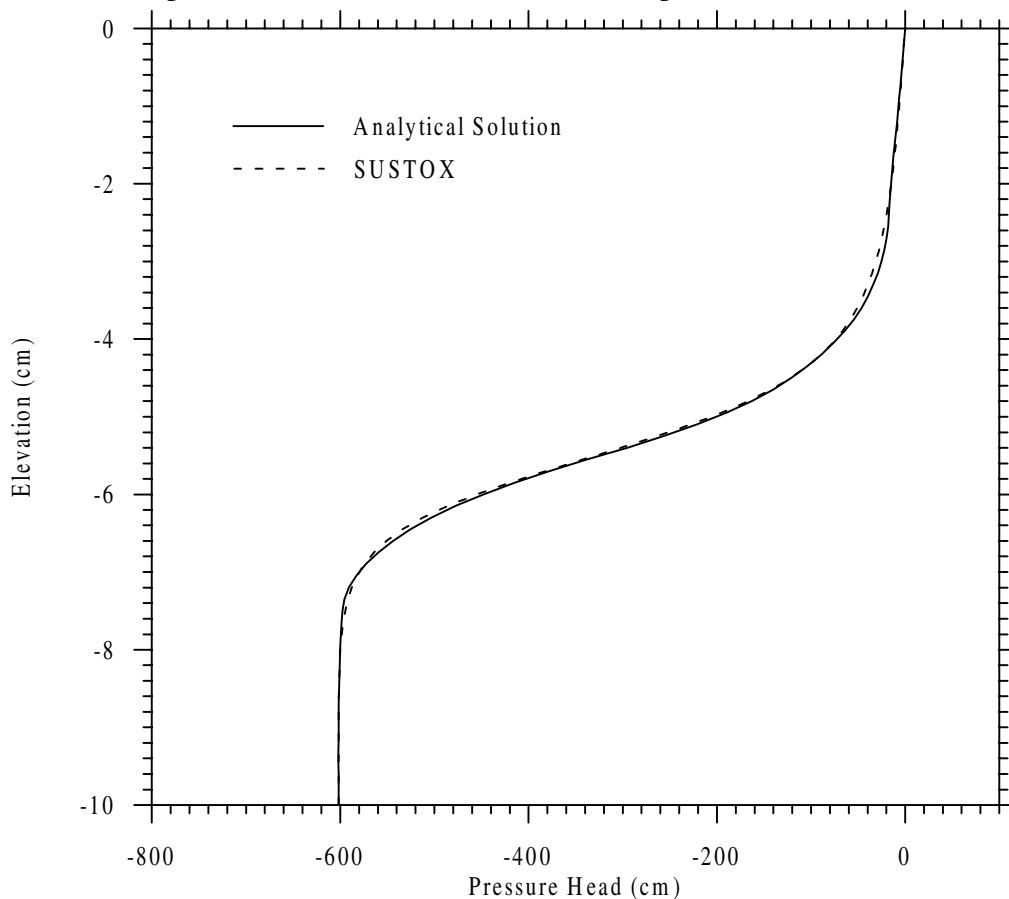


Figure 2. Comparison of SUSTOX numerical results with semi-analytic solution for Philip's infiltration problem after 2.0 hours of infiltration.

Transport processes include both advection and hydrodynamic dispersion as functions of moisture content. Semi-analytical solution for the one-dimensional flow domain represented in this unsaturated transport problem was provided by Philip [13]. Semi-analytic solution for same transport problem was obtained by Smiles et al. [14].

A saturation commencing at time zero is assigned on the left boundary of 20-cm horizontal soil tube, and a constant liquid pressure of 93,157.21 Pa was specified on the right boundary. The species boundary conditions are 1.0 g/L species concentration commencing at time zero at the left boundary and 0.1 g/L at the right boundary. The initial conditions are a liquid pressure of 93,157.21 Pa and species liquid concentration of 0.1 g/L. Values of other parameters used in simulations are given in Table 2.

Comparison between SUSTOX solution and semi-analytic solution at various time moments are shown in Figure 3 as dash and solid lines, respectively. Solute concentration obtained by SUSTOX code is converted into a dimensionless concentration by scaling it between the values at each boundary using a formulae $c=(c-c^n)/(c^0-c^n)$.

The SUSTOX input file for unsaturated species transport problem is given in appendix B.

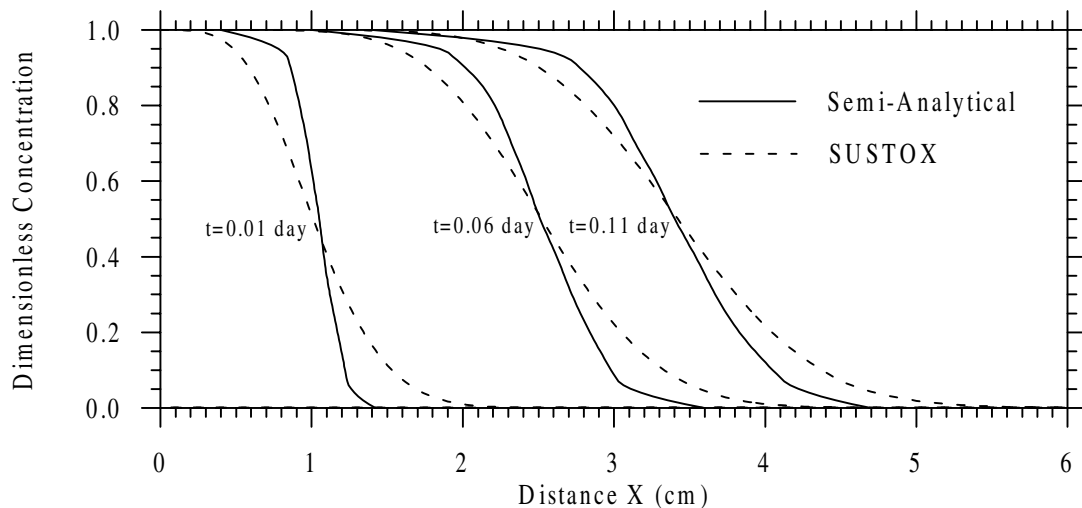


Figure 3. Comparison between dimensionless solute concentrations versus distance at various times generated by semi-analytic solution and SUSTOX code.

6 Radionuclides Migration in the Subsurface around the Chernobyl NPP

6.1 Site Description

A Shelter containment structure constructed upon the ruins of the destroyed reactor building of the Chernobyl Unit-4 was completed in November 1986. This containment has been built in very high radioactive fields in the short time span of six months by using of unique and remote construction methods. However, these remote methods for pouring fresh concrete did not always permit observation and review of work, and in a number of cases high radioactive fields made welding key containment components impossible. As a result of these construction difficulties, area of openings and breaks in the walls and the roof of the Shelter is estimated to total about 1200 m².

By current estimates, the Shelter contains from 135 to 180 tons of nuclear fuel with an activity of up to 20,000,000 Ci [15]. Within the Shelter the largest part of the nuclear fuel from the completely destroyed reactor core is contained in fuel-containing materials (FCM), and the rest in fuel assemblies and their fragments. The FCM can be represented as lava-like materials with a glass silicate matrix containing many inclusions of various uranium compounds, finely dispersed high-level active fuel dust, and aerosols. Experimental observations show a gradual increase in the migration rate of radionuclides from the FCM caused by its permanent interaction with water and atmosphere inside the Shelter. Contamination of the environment by radioactive substances from the Shelter may occur in two principal ways: (1) the release of fuel dust into the atmosphere through openings in the Shelter if there is a collapse of internal structures within the Shelter, and (2) the migration of radionuclides through the subsurface together with water which is inside the Shelter.

According to previous research [16-17] the Shelter contains more than 3,000 m³ of intermediate-level and low-level radioactive water. More than 1,000 m³ of intermediate-

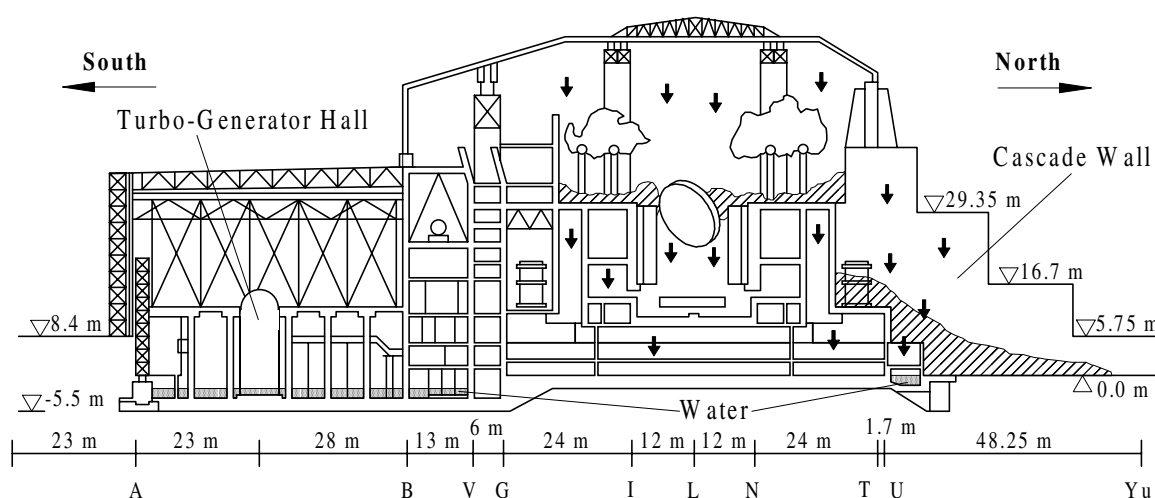


Figure 4. Schematic of the Chernobyl Unit-4 Shelter, water pathways and locations within the Shelter. North-South Cross-Section along Axis 47.

level radioactive water is disposed in the basement of the Unit-4. Most of contaminated water is located in the turbo-generator hall and rooms on the first level in the northern part of the Shelter (Figure 4). It is also reasonable to consider such major water sources within the Shelter as: precipitation, water used for dust suppression, moisture condensation onto building structures, and water leakage from the service lines of the 3rd unit of the Chernobyl NPP. Most precipitation onto the roof penetrates through cracks to the interior of the Shelter. The volume of this precipitation is approximately $1,000 \text{ m}^3$ per year. For dust suppression, 15 m^3 of water are sprayed twice a month within the Shelter. Water enters the Shelter through the above mentioned openings and flows downwards both into the lower regions of the reactor building and through the cascade wall where most of the fuel is located. Upon movement through the FCM and interaction with FCM, the water is contaminated by radionuclides. The contaminated water penetrates to the subsurface environment. The total activity of the intermediate-level radioactive water lies within the range of 2×10^{12} to $9 \times 10^{13} \text{ Bq/l}$. Caesium isotopes constitute the main portion of the water activity; the caesium activity varies from 1.6×10^5 to $5.5 \times 10^7 \text{ Bq/l}$. The total ^{90}Sr activity in the water was determined to be 3.6×10^3 to $1.1 \times 10^6 \text{ Bq/l}$.

The Chernobyl NPP is located on the right bank of the Pripjat River. The NPP site is a flat river bench. The aquifer system is composed of fine, medium and sometimes coarse alluvial sands with interlayers of sand loam and loam. Medium sands prevail. According to field studies the hydraulic conductivity of the alluvial sands ranges from 6.0 to 15.0 m day^{-1} . These alluvial sands lie above 25 to 40 m of clay marls of the Kiev Eocene suite. The marls have very low permeability and act as an aquitard. The infiltration is estimated between 80 mm and 200 mm per year [15,18].

6.2 Simulation Results

Numerical simulations of the ^{90}Sr and ^{137}Cs migration from the Shelter into and through the subsurface environment were conducted for a two-dimensional vertical cross section selected along the streamlines of groundwater flow. These streamlines were obtained from field observations of groundwater level distribution in the vicinity of the Chernobyl NPP. The geology of this cross section is shown in Figure 5.

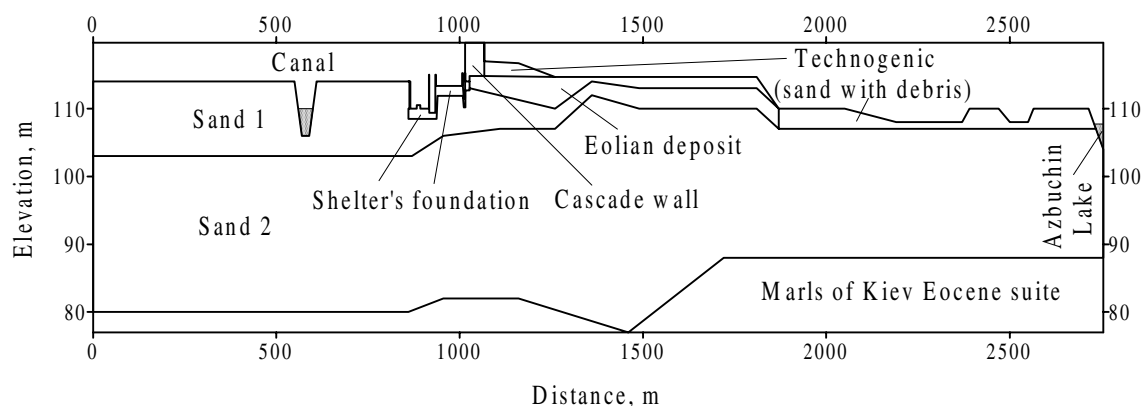


Figure 5. Schematic representation of geologic section.

Table 3. Values of Parameters Used in Numerical Simulations.

Soil or Rock	K m day ⁻¹	n_T	ρ_s gm cm ⁻³	α_L m	α_T m	k_d^{Sr} L kg ⁻¹	k_d^{Cs} L kg ⁻¹	α_{sf}^{Cs} day ⁻¹	α_{fs}^{Cs} day ⁻¹
Eolian deposit	13.	0.316	2.34	1.2	0.1	1.0	5.2	0.001	0.00005
Sand 1	9.	0.35	2.46	1.2	0.1	1.0	5.2	0.001	0.00005
Sand 2	10.	0.342	2.43	1.2	0.1	1.0	5.2	0.001	0.00005
Cascade Wall	1.	0.12	2.1	1.0	0.1	0.5	5.2	0.001	0.00005
Concrete	0.001	0.06	2.66	1.	0.1	0.5	5.2	0.001	0.00005
Technogenic	11.	0.36	2.5	1.2	0.1	1.0	5.2	0.001	0.00005

The flow domain was discretized by a non-uniform rectangle mesh, nodes of which spaced at 1 to 100 m intervals in the horizontal direction, and 0.2 to 3 m in the vertical direction. Time steps of 30 days were used. Values for the hydraulic and species properties used in the simulations are given in Table 3. Values of the first-rate constants α_{sf} , α_{fs} were taken similar to experimentally obtained values of these parameters for upper soil layer of left bank floodplain of Pripyat river. Parameters α_{sf} and α_{fs} vanish for the case of ⁹⁰Sr migration in the subsurface. The coefficient of radionuclide leaching from fuel particles was 3.2×10^{-4} day⁻¹ [15].

The prescribed values of hydraulic head were specified along the left and right boundaries, the top of the Shelter's foundation, and boundaries on which surface water bodies are intercepted by the aquifer. At the ground surface liquid flow rate was equal to infiltration or evapotranspiration rate. Annual amount of infiltration was 80 mm. The marls were considered as impervious. Water depth was assumed to be 2 m in turbo-generator hall, and 1.6 m in rooms on the first level in the northern part of the Shelter. Seasonal fluctuations of the water level in the canal varied between 109.5 m and 110.2 m; in Azbuchin Lake, between 106.0 m and 106.8 m; and for the hydraulic head at the left boundary, between 109.5 m and 110.0 m [18]. These seasonal fluctuations of water level in surface water bodies and the variability over time of precipitation and evapotranspiration were taken into account in the simulations.

Before Chernobyl accident a special drainage system operated to prevent underflooding of the Chernobyl NPP building's foundation. After Chernobyl accident this drainage system was damaged and shut down. In result of that groundwater level increase was observed until 1994. Nowadays groundwater level below the Shelter varies from 109.5 m to 110.5 m in dependence on seasonal groundwater fluctuations and precipitation. The groundwater increase after Chernobyl accident was not taken into account in simulations. The initial condition for the liquid phase is illustrated in Figure 6.

A zero radionuclide flux condition was employed at all boundaries, excluding the Shelter basement and boundaries that contact surface water bodies. The ⁹⁰Sr activity of water from the basement was 2.3×10^6 Bq/l, and 2800 Bq/l in Azbuchin Lake [19]. Similarly, ¹³⁷Cs activity in the basement water and Azbuchin Lake were 7.1×10^7 and 84 Bq/l, respectively. From 1986 to 1995, the radionuclide activity of canal water was assigned the annual average activity of water samples from Cooling pond. The radionuclide activity of canal water after 1995 was specified as the radionuclide activity of canal water in 1995. For the area surrounding the Chernobyl NPP, land surface contamination by ¹³⁷Cs in 1995 was from 3.8×10^{-4} to 1.9×10^{-6} Ci per kg of soil. ⁹⁰Sr land

surface contamination was equal to one half of ^{137}Cs land surface contamination. Just after the accident, exchangeable ^{90}Sr was 5% of the total ^{90}Sr activity and exchangeable ^{137}Cs was 10% of the total ^{137}Cs activity. The subsurface was assumed to be uncontaminated before the accident. The date of the Chernobyl accident was taken as the start date for the simulations.

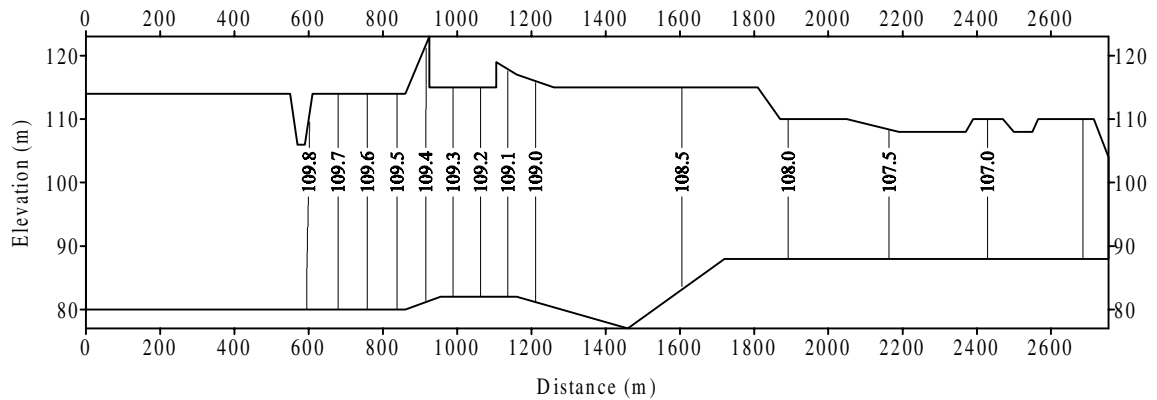


Figure 6. Initial hydraulic head distribution.

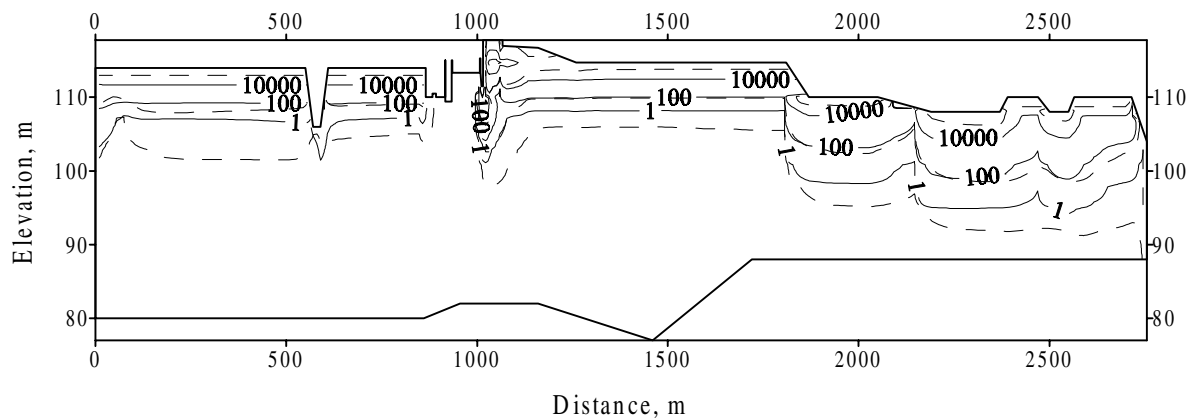


Figure 7. Activity of ^{90}Sr (Bq/l) in the aqueous phase in (—) 1995 and (- - -) 2045 for case 2.

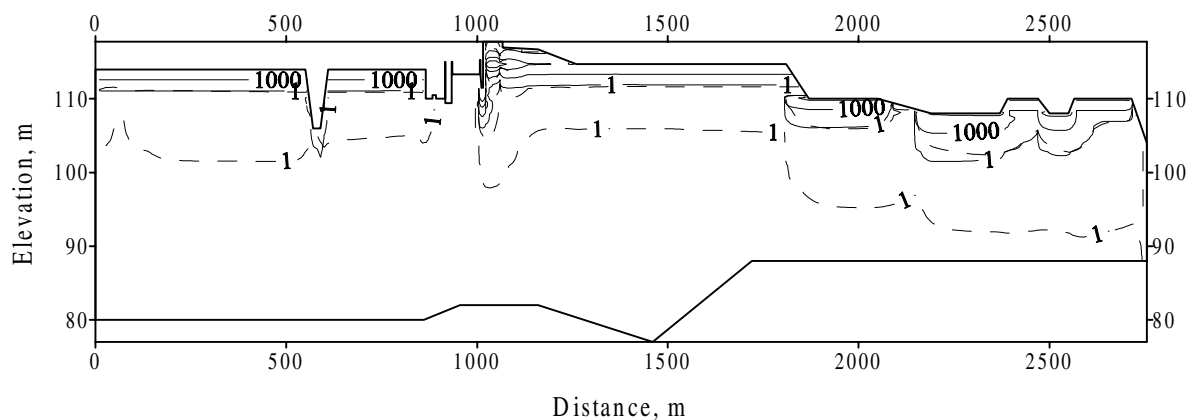


Figure 8. Activity of ^{137}Cs (Bq/l) in the aqueous phase in (—) 1995 and (- - -) 2045 for case 2.

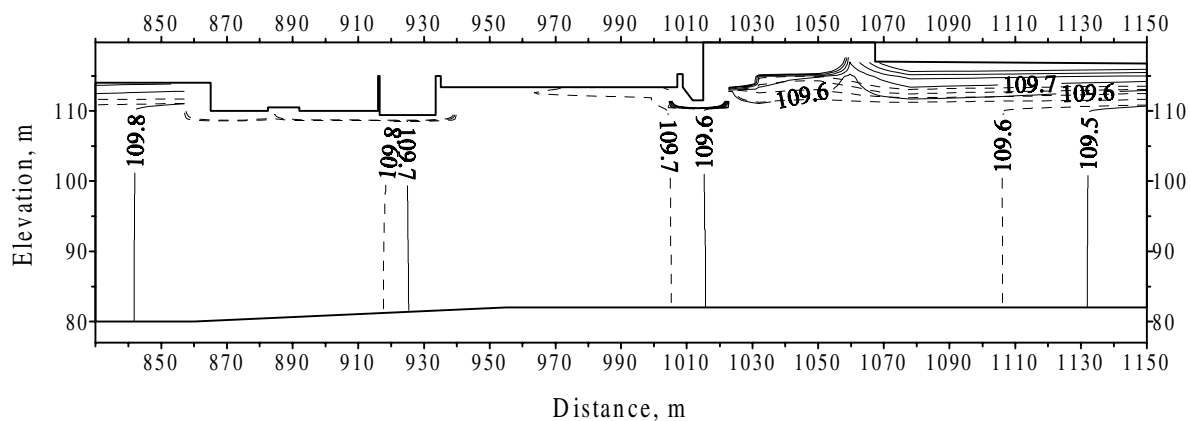


Figure 9. Summer distribution of hydraulic head below the Shelter for (—) case 2 and (- - -) case 3.

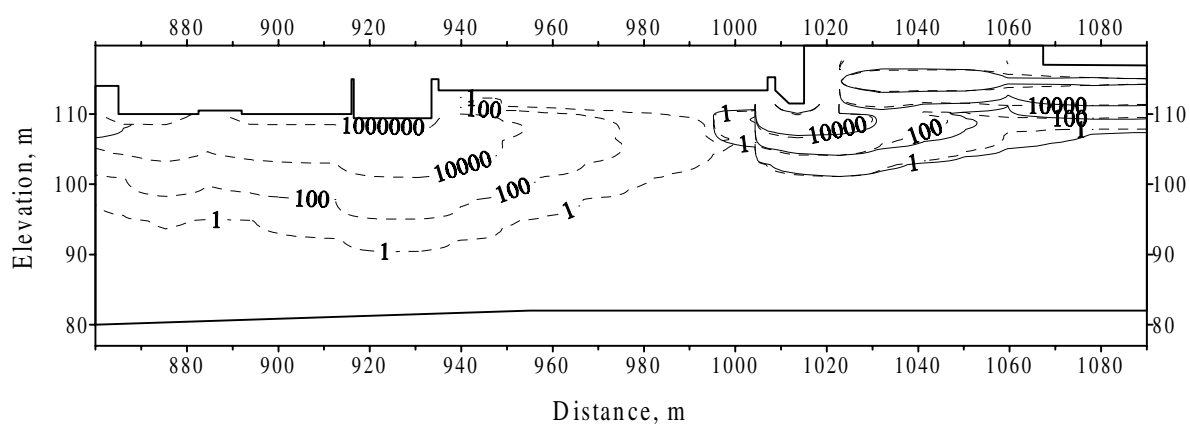


Figure 10. Activity of ^{90}Sr (Bq/l) in the aqueous phase below the Shelter in 1995 for (—) case 2 and (- - -) case 3.

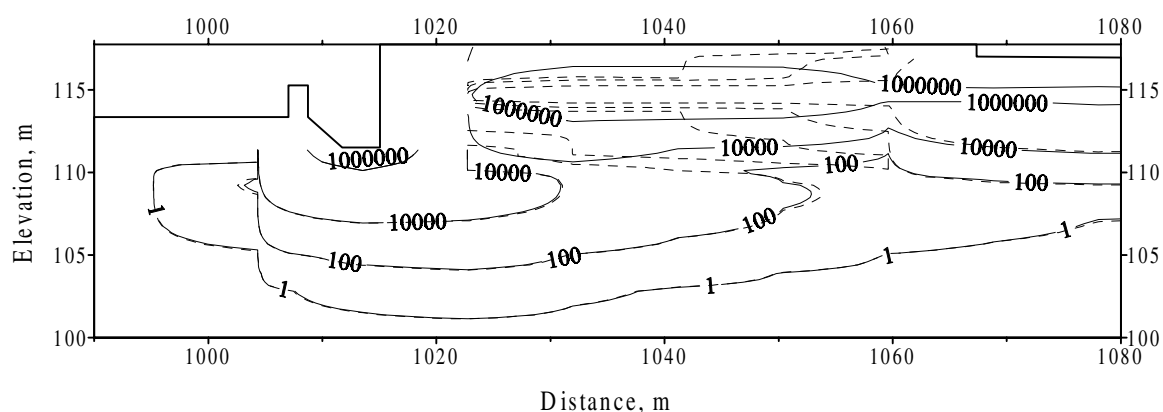


Figure 11. Activity of ^{90}Sr (Bq/l) in the aqueous phase below the Shelter in 1995 for (—) case 2 and (- - -) case 1.

There are no reliable data on water leakage to outside the bounds of the Shelter. However, analysis of water pathways and water locations within the Shelter shows that there is possibility of water leakage from the turbo-generator hall, northern rooms of the Shelter, and through the cascade wall. The cascade wall was filled with concrete, boxed radioactive materials collected from the roof and surroundings, building debris, and structural metals. So, it has a lot of openings and breaks through which part of precipitation onto the cascade wall penetrates to the subsurface. Therefore, in order to estimate migration rates of radionuclides from the Shelter through the subsurface, numerical simulations were conducted for following cases:

Case 1. Water leakage occurs from rooms on the first level in the northern part of the Shelter.

Case 2. In addition to case 1, one half precipitation onto the cascade wall penetrates to outside of the Shelter.

Case 3. Waters from turbo-generator hall, rooms in the northern part of the Shelter, and half precipitation onto the cascade wall penetrate to the subsurface environment.

The effects of various water leakage scenarios on radionuclide migration from the Shelter through the subsurface are compared to case 2. Figures 6-8 show the predicted activity distribution of ^{90}Sr and ^{137}Cs radionuclides in the aqueous phase in 1995 and 2045 for case 2.

The influence of different water leakage to outside of the Shelter on migration of ^{90}Sr through the subsurface is shown in Figures 9-11. Analysis of the results indicates a slight increase of groundwater level and radionuclide migration rate below the Shelter for case 3. The effect of water penetration through the cascade wall on radionuclide migration below the Shelter is negligible.

Comparisons of predicted activity depth profiles of ^{90}Sr and ^{137}Cs radionuclides in the aqueous phase with measurements in 1995 are given in Figures 12 and 13. These predicted activity-depth profiles were selected at point $x=1075$ m which approximately correspond to location of wells 1-g, 2-g and 4-g in the northern part of the Chernobyl NPP building area. Annual mean values of radionuclide activity obtained on measurements in the wells 1-g, 2-g, 4-g and 6-g [16] are denoted by circles. Triangle denotes the radionuclide activity detected in well C10 in 1995 [19]. The well C10 is located in 150-200 m to the east of the wells 1-g and 4-g.

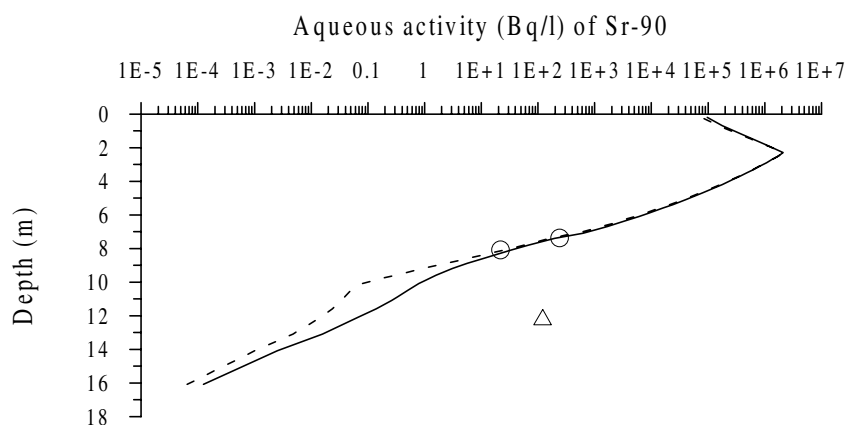


Figure 12. Comparison of predicted and measured activity-depth profiles of ^{90}Sr in the aqueous phase in 1995. Model-generated profiles were obtained for (—) case 2 and (- - -) case 3. Δ and O denote mean values of radionuclide activity detected in well C10 and in wells 1-g, 2-g, 4-g and 6-g, respectively.

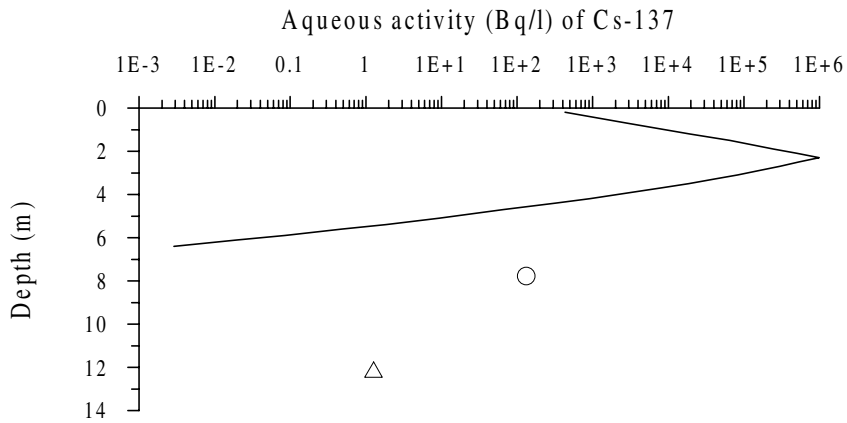


Figure 13. Comparison of predicted and measured activity-depth profiles of ^{137}Cs in the aqueous phase in 1995. Model-generated profile was obtained for (—) case 2. Δ and O denote mean values of radionuclide activity detected in well C10 and in wells 1-g, 2-g, 4-g and 6-g, respectively.

7 Input File Structure

Structure of SUSTOX Input file is similar to MST5 Input file structure [20-21].

7.1 Simulation Title Card

The Simulation Title card is used to specify information that identifies an Input file, including the title of the simulation, the user's name and affiliation, date and time of Input file creation, and any notes the user may enter.

Format:

Line 0 “~Simulation Title and Notes”
Line 1 Simulation Title {character*80}
Line 2 User Name {character*80}
Line 3 Company Name {character*40}
Line 4 Input File Creation Date {character*40}
Line 5 Input File Creation Time {character*40}
Line 6 N {integer} “line(s) of simulation title notes follows.”
Line n Simulation Title Notes {character*120}

7.2 Solution Schemes Card

The Solution Scheme card is used to restart options, control simulation time variables, and specify which governing equations to solve.

Format:

Line 0 “~Solution Schemes”
Line 1 Initial Conditions Only [true | false],
 Restart [true | false],
 Restart from Time Zero [true | false],
Line 2 Water Equation [true | false],
 Species Transport Equation [true | false],
Line 3 Simulation Time Limit,
 Units [s | min | h | day | wk | yr],
Line 4 Initial Time Step,
 Units [s | min | h | day | wk | yr],
Line 5 Time Step Acceleration Factor,
Line 6 Maximum Time Step,
 Units [s | min | h | day | wk | yr],
Line 7 Screen Echo [true | false],

7.3 Numerical Control Card

The Numerical Control card is used to control the iteration process, and specify the numerical convergence limits and averaging technique used for solution of each of the governing equations.

Format:

- Line 0 “~Numerical Control”
- Line 1 Number of Newton Iterations,
Residuals Convergence [maximum residual | least squares]
- Line 2 Criterion Error Tolerance of Water Equation Convergence,
- Line 3 Water Equation Mean [harmonic | geometric | arithmetic | upwind],

7.4 Grid Geometry Card

The Grid Geometry card is used to specify the number of nodes in each Cartesian direction, specify the physical length of the problem domain, and indicate the physical location of all nodes in the problem domain. The problem domain is discretized into a computational domain composed of non-overlapping node volumes. Node volumes are defined by their bounding surfaces. Surfaces between nodes are located at the midpoint between two adjacent nodes. Grid geometry should arrange a grid such that the lower and upper boundaries of problem domain are a bounding surfaces of node volumes, and the lower grid boundary in each dimension is at position zero. Node positions are referenced from the west, south, or bottom boundaries for the x -, y -, and z -coordinate directions.

Format:

- Line 0 “~Grid Geometry”
- Line 1 Number of Grid Nodes in the X-direction,
Number of Grid Nodes in the Y-direction,
Number of Grid Nodes in the Z-direction,
- Line 2 Physical Domain Length in X-direction,
Units [m | ft | cm],
Physical Domain Length in Y-direction,
Units [m | ft | cm],
Physical Domain Length in Z-direction,
Units [m | ft | cm],
Z-direction Datum,
Units [m | ft | cm],
Z-direction Grid Bottom Elevation from Datum,
Units [m | ft | cm],
- Line 3 I {integer} “line(s) of grid geometry input follows.”
- Line i “Node “ i {integer},
X-direction Node Position,
Units [m | ft | cm],
- Next Line J {integer} “line(s) of grid geometry input follows.”
- Line j “Node “ i {integer},
Y-direction Node Position,
Units [m | ft | cm],
- Next Line K {integer} “line(s) of grid geometry input follows.”
- Line k “Node “ i {integer},
Z-direction Node Position,

Units [m | ft | cm],

7.5 Inactive Nodes Card

The Inactive Nodes card is used to designate inactive, non-computational nodes in the problem domain. Often the rectangular grid required by the finite difference method does not provide the flexibility needed to describe complex geometry. The inactive nodes feature gives some flexibility in this regard.

Format:

Line 0 “~Inactive Nodes”
Line 1 N {integer} “line(s) of inactive nodes input follows.”
Line n I Start {integer},
 I End {integer},
 J Start {integer},
 J End {integer},
 K Start {integer},
 K End {integer},

7.6 Rock or Soil Types Card

The Rock or Soil Types card is used to group computational nodes with identical physical properties into unique rock or soil types.

Format:

Line 0 “~Rock or Soil Types”
Line 1 N {integer} “line(s) of rock or soil types notes follows.”
Line n Rock Notes {character*120}
Next N {integer} “line(s) of rock or soil types input follows.”
Line
Line n Rock or Soil Type {character*80},
 I Start {integer},
 I End {integer},
 J Start {integer},
 J End {integer},
 K Start {integer},
 K End {integer},

7.7 Mechanical Properties Card

The Mechanical Properties card is used to assign values of porosity, density, tortuosity, longitudinal and transverse dispersivities to rock or soil types identified with the Rock or Soil Types card.

Format:

Line 0 “~Mechanical Properties”
Line 1 N {integer} “line(s) of mechanical properties input follows.”

Units [L^2/T],
 Solid-Liquid Partition Coefficient {real},
 Units [M liq./ M sol.],
 Species Half-Life {real},
 Units [s | min | h | day | wk | yr],
 Slow Sorption Rate {real},
 Units [1/s | 1/min | 1/h | 1/day | 1/wk | 1/yr],
 Slow Desorption Rate {real},
 Units [1/s | 1/min | 1/h | 1/day | 1/wk | 1/yr],

where unit of M is [kg | gm | lbm]; unit of T is [min | h | day | s | wk | yr]; and unit of L is [m | cm | mm | in | ft | yd].

7.10 Soil Characteristics Card

Soil Characteristics card is used to specify the relationship between liquid pressure and liquid saturation for unsaturated conditions for each rock or soil types identified with the Rock or Soil Types card.

Format:

Line 0 “~Soil Characteristics”
 Line 1 N {integer} “line(s) of soil characteristics input to follow.”

van Genuchten relation

Line n Rock or Soil Type {character*80},
 “van Genuchten”,
 van Genuchten α parameter {real},
 Units [1/cm | 1/m | 1/ft],
 van Genuchten n parameter ,
 Maximum Tension Head {real},
 Units [m | ft | cm],
 ,
 ,

Brooks and Corey relation

Line n Rock or Soil Type {character*80},
 “Brooks and Corey”,
 Brooks and Corey ψ^* parameter {real},
 Units [m | ft | cm],
 Brooks and Corey m parameter {real},
 Maximum Tension Head {real},
 Units [m | ft | cm],
 ,
 ,

Haverkamp relation

Line n Rock or Soil Type {character*80},
 [“Haverkamp 1” | “Haverkamp 2”],

Haverkamp α parameter {real},
 ,
 Haverkamp β parameter {real},
 Maximum Tension Head {real},
 Units [m | ft | cm],
 ,
 ,

Tabular data

Line n Rock or Soil Type {character*80},
 "Tabular",
 Table No." N {integer},
 ,
 ,
 ,
 ,

Tables for tabular data follow all functional input lines. Tables must be ordered sequentially according to their respective table numbers.

Line 1 N {integer} "line(s) of capillary tables input follows."
 Line n Tension Head {real},
 Liquid Saturation {real},
 Tension Head Units [m | ft | cm],

7.11 Liquid Relative Permeability Card

The Liquid Relative Permeability card is used to specify the relationship between liquid relative permeability and liquid saturation or between liquid relative permeability and capillary pressure head for unsaturated conditions for each rock or soil types identified with the Rock or Soil Types card.

Format:

Line 0 "~Liquid Relative Permeability Properties"
 Line 1 N {integer} "line(s) of liquid relative permeability input to follow."

Mualem function with van Genuchten soil-moisture-retention relation.

Line n Rock or Soil Type {character*80},
 "Mualem w/ van Genuchten",
 van Genuchten *m* parameter {real},
 ,
 Minimum Liquid Relative Permeability {real},

Mualem function with Brooks and Corey soil-moisture- retention relation.

Line n Rock or Soil Type {character*80},
 "Mualem w/ Brooks&Corey",
 Brooks and Corey *m* parameter {real},
 ,
 Minimum Liquid Relative Permeability {real},

Burdine function with van Genuchten soil-moisture-retention relation.

Line n Rock or Soil Type {character*80},
 “Burdine w/ van Genuchten”,
 van Genuchten m parameter {real},
 ,
 Minimum Liquid Relative Permeability {real},

Burdine function with Brooks and Corey soil-moisture- retention relation.

Line n Rock or Soil Type {character*80},
 “Burdine w/ Brooks&Corey”,
 Brooks and Corey m parameter {real},
 ,
 Minimum Liquid Relative Permeability {real},

Haverkamp relation.

Line n Rock or Soil Type {character*80},
 “Haverkamp”,
 Haverkamp A parameter {real},
 Haverkamp B parameter {real},
 Minimum Liquid Relative Permeability {real},

Touma and Vauclin relation.

Line n Rock or Soil Type {character*80},
 “Touma and Vauclin”,
 Fitting A parameter {real},
 Fitting B parameter {real},
 Minimum Liquid Relative Permeability {real},

Tabular versus Liquid Saturation

 Rock or Soil Type {character*80},
 “Tabular vs Liquid Saturation”,
 “Table No. “ M {integer},
 ,
 ,

Tables for tabular data follow all functional input lines. Tables must be ordered sequentially according to their respective table numbers.

Line 1 N {integer} “line(s) of liquid permeability tables input follows.”
Line n Liquid Saturation {real},
 Liquid Relative Permeability {real},

Tabular versus Tension Head

Line n Rock or Soil Type {character*80},
 “Tabular vs Tension Head”,
 “Table No. “ M {integer},
 ,
 ,

Tables for tabular data follow all functional input lines. Tables must be ordered sequentially according to their respective table numbers.

Line 1 N {integer} “line(s) of liquid permeability tables input follows.”
Line n Tension Head {real},
Liquid Relative Permeability {real},
Tension Head Units [m | ft | cm],

7.12 Liquid Boundary Conditions Card

The Liquid Boundary Conditions card is used to specify the boundary conditions for liquid pressure, hydraulic head, and liquid fluxes at the external boundaries of the problem domain and at the boundaries of inactive nodes.

Format:

Line 0 “~Liquid Boundary Conditions”
Line 1 N {integer} “line(s) of liquid boundary conditions input to follow.”

Dirichlet Boundary

Line n Direction [X-Direction | Y-Direction | Z-Direction]:
Surface [Top | Bottom | East | West | North | South] “ Surface”,
“Dirichlet @ Boundary”,
Temporal Variation [constant | tabular],

Constant

Liquid Pressure {real},
Units [Pa (absolute) | Psi (absolute) | Atm (absolute) | Bar (absolute)],
I Start {integer},
I End {integer},
J Start {integer},
J End {integer},
K Start {integer},
K End {integer},

Tabular

Table Name {character*20},
,
I Start {integer},
I End {integer},
J Start {integer},
J End {integer},
K Start {integer},
K End {integer},

Neumann Boundary.

Line n Direction [X-Direction | Y-Direction | Z-Direction]:
Surface [Top | Bottom | East | West | North | South] “ Surface”,
“Neumann @ Boundary”,

Temporal Variation [constant | tabular],

Constant

Liquid Mass Flux {real},
Units [$M/L^2 T$],
I Start {integer},
I End {integer},
J Start {integer},
J End {integer},
K Start {integer},
K End {integer},

Tabular

Table Name {character*20},
,
I Start {integer},
I End {integer},
J Start {integer},
J End {integer},
K Start {integer},
K End {integer},

where unit of M is [kg | gm | lbm]; unit of T is [min | h | day | s | wk | yr]; and unit of L is [m | cm | mm | in | ft | yd].

Hydraulic Head Boundary

Line n Direction [X-Direction | Y-Direction | Z-Direction]:
 Surface [Top | Bottom | East | West | North | South] “ Surface”,
 “Hydraulic Head @ Boundary”,
 Temporal Variation [constant | tabular],

Constant

Hydraulic Head {real},
Units [m | ft | cm],
I Start {integer},
I End {integer},
J Start {integer},
J End {integer},
K Start {integer},
K End {integer},

Tabular

Table Name {character*20},
,
I Start {integer},
I End {integer},
J Start {integer},
J End {integer},

K Start {integer},
K End {integer},

Tables for tabular data follow all functional input lines. Tables must be in ascending or descending order.

Line 1 N {integer} “line(s) of all boundary tables input follows.”

Line n Time {real},
Units [s | min | h | day | wk | yr],
Boundary Value {real},
Boundary Value Units,

7.13 Species Boundary Conditions Card

The Species Boundary Conditions card is used to specify the boundary conditions for species concentrations and species boundary surface fluxes at the external boundaries of the problem domain and at the boundaries of inactive nodes.

Format:

Line 0 “~Species Boundary Conditions”

Line 1 N {integer} “line(s) of species boundary conditions input to follow.”

Dirichlet Boundary

Line n Direction [X-Direction | Y-Direction | Z-Direction]:
Surface [Top | Bottom | East | West | North | South] “ Surface”,
“Dirichlet @ Boundary”,
Temporal Variation [constant | tabular],

Constant

Liquid-Phase Species Concentration {real},
Units [1/L³],
I Start {integer},
I End {integer},
J Start {integer},
J End {integer},
K Start {integer},
K End {integer},

where unit of *L* is [m | cm | mm | in | ft | yd].

Tabular

Table Name {character*20},
,
I Start {integer},
I End {integer},
J Start {integer},
J End {integer},
K Start {integer},
K End {integer},

Neumann Boundary

Line n Direction [X-Direction | Y-Direction | Z-Direction]:
 Surface [Top | Bottom | East | West | North | South] “ Surface”,
 “Neumann @ Boundary”,
 Temporal Variation [constant | tabular],

Constant

Liquid-Phase Species Flux {real},
Units [1/L² T],
I Start {integer},
I End {integer},
J Start {integer},
J End {integer},
K Start {integer},
K End {integer},

Tabular

Table Name {character*20},
,
I Start {integer},
I End {integer},
J Start {integer},
J End {integer},
K Start {integer},
K End {integer},

where unit of T is [min | h | day | s | wk | yr]; and unit of L is [m | cm | mm | in | ft | yd].

Outflow Boundary

Line n Direction [X-Direction| Y-Direction| Z-Direction]:
 Surface [Top|Bottom|East|West|North|South] “ Surface”,
 “Outflow @ Boundary”,
,
,
,
I Start {integer},
I End {integer},
J Start {integer},
J End {integer},
K Start {integer},
K End {integer},

Tables for tabular data follow all functional input lines. Tables must be in ascending or descending order.

Line 1 N {integer} “line(s) of all boundary tables input follows.”
Line n Time {real},
 Units [s | min | h | day | wk | yr],
 Boundary Value {real},

Boundary Value Units,

7.14 Fuel Particle Sources Card

The Fuel Particle Sources card is used to specify initial contamination of problem domain by fuel particle, and portions of the exchangeable and fixed phases in this contamination.

Format:

Line 0 “~Fuel Particle Sources”
Line 1 N {integer} “line(s) of fuel particle sources input to follow.”
Line n Fuel Particle Concentration {real},
 Unit [1/L³],
 Radionuclide Leaching Rate {real},
 Unit [1/s | 1/min | 1/h | 1/day | 1/wk | 1/yr],
 Exchangeable-phase portion in fuel contamination {real},
 Fixed-phase portion in fuel contamination {real},
 I Start {integer},
 I End {integer},
 J Start {integer},
 J End {integer},
 K Start {integer},
 K End {integer},

where unit of L is [m | cm | mm | in | ft | yd].

7.15 Initial Conditions Card

The Initial Conditions card is used to specify the values of field variables at the computational nodes at the start of a simulation. No field variable initial conditions are required for restart simulations.

Format:

Line 0 “~Initial Conditions”
Line 1 N {integer} “line(s) of initial conditions input to follow.”
Line n Variable Name [Liquid Pressure | Hydraulic Head | Species Concentration |
 Species Liquid Concentration | X-Dir. Liquid Velocity | Y-Dir. Liquid
 Velocity | Z-Dir. Liquid Velocity],
 Field Variable Value {real},
 Units *Pressure*. [Pa (absolute) | Psi (absolute) | Atm (absolute) | Bar
 (absolute)],
 Hydraulic Head. [m | ft | cm],
 Concentration. [1/L³ | 1/V],
 X-Direction Gradient {real},
 Units [1/m | 1/ft | 1/cm],
 Y-Direction Gradient {real},
 Units [1/m | 1/ft | 1/cm],

Z-Direction Gradient {real},
Units [1/m | 1/ft | 1/cm],
I Start {integer},
I End {integer},
J Start {integer},
J End {integer},
K Start {integer},
K End {integer},

where unit of V is [liter | l | gal]; and unit of L is [m | cm | mm | in | ft | yd].

7.16 Sources and Sinks Card

The Sources and Sinks card is used to identify the location and rate of sources and/or sinks of liquid mass and species mass. The source/sink rate either may be constant in time or may vary following tabular input.

Format:

Line 0 “~Sources & Sinks”
Line 1 N {integer} “line(s) of sources & sinks input to follow.”
Line n Source Type [Liquid Mass | Species | Species Concentration | Species Liq Concentration]

Liquid Mass

Source Temporal Variation [Constant | Tabular],

Constant

Liquid Source Rate {real},
Units [M/T],
Source Start Time {real},
Units [s | min | h | day | wk | yr],
Source End Time {real},
Units [s | min | h | day | wk | yr],
I Start {integer},
I End {integer},
J Start {integer},
J End {integer},
K Start {integer},
K End {integer},

where unit of M is [kg | gm | lbm]; and unit of T is [min | h | day | s | wk | yr].

Tabular

Table number {integer},
,
,
I Start {integer},
I End {integer},

J Start {integer},
 J End {integer},
 K Start {integer},
 K End {integer},
 Line n M {integer} "line(s) of source tables input follows."
 Line m Time {real},
 Units [s | min | h | day | wk | yr],
 Liquid Mass Source Rate {real},
 Units [M/T],

where unit of M is [kg | gm | lbm]; and unit of T is [min | h | day | s | wk | yr].

Species

Source Temporal Variation [Constant | Tabular],

Constant

Species Source Rate {real},
 Units [1/s | 1/min | 1/h | 1/day | 1/wk | 1/yr],
 Source Start Time {real},
 Units [s | min | h | day | wk | yr],
 Source End Time {real},
 Units [s | min | h | day | wk | yr],
 I Start {integer},
 I End {integer},
 J Start {integer},
 J End {integer},
 K Start {integer},
 K End {integer},

Tabular

Table number {integer},
 ,
 ,
 I Start {integer},
 I End {integer},
 J Start {integer},
 J End {integer},
 K Start {integer},
 K End {integer},
 Line n M {integer} "line(s) of source tables input follows."
 Line m Time {real},
 Units [s | min | h | day | wk | yr],
 Species Mass Source Rate {real},
 Units [M/T],

where unit of M is [kg | gm | lbm]; and unit of T is [min | h | day | s | wk | yr].

Species Concentration

Source Temporal Variation [Constant | Tabular],

Constant

Species Concentration Source Rate {real},
Units [$1/L^3 T$],
Source Start Time {real},
Units [s | min | h | day | wk | yr],
Source End Time {real},
Units [s | min | h | day | wk | yr],
I Start {integer},
I End {integer},
J Start {integer},
J End {integer},
K Start {integer},
K End {integer},

where unit of T is [min | h | day | s | wk | yr]; and unit of L is [m | cm | mm | in | ft | yd].

Tabular

Table number {integer},
,
,
I Start {integer},
I End {integer},
J Start {integer},
J End {integer},
K Start {integer},
K End {integer},

Line n M {integer} “line(s) of source tables input follows.”

Line m Time {real},
Units [s | min | h | day | wk | yr],
Species Mass Concentration Source Rate {real},
Units [$M/L^3 T$],

where unit of M is [kg | gm | lbm]; unit of T is [min | h | day | s | wk | yr]; and unit of L is [m | cm | mm | in | ft | yd].

Species Liquid Concentration

Source Temporal Variation [Constant | Tabular],

Constant

Species Liquid Concentration Source Rate {real},
Units [$1/L^3 T$],
Source Start Time {real},
Units [s | min | h | day | wk | yr],
Source End Time {real},

Units [s | min | h | day | wk | yr],
 I Start {integer},
 I End {integer},
 J Start {integer},
 J End {integer},
 K Start {integer},
 K End {integer},

where unit of T is [min | h | day | s | wk | yr]; and unit of L is [m | cm | mm | in | ft | yd].

Tabular

Table number {integer},
 ,
 ,
 I Start {integer},
 I End {integer},
 J Start {integer},
 J End {integer},
 K Start {integer},
 K End {integer},

Line n M {integer} “line(s) of source tables input follows.”
 Line m Time {real},
 Units [s | min | h | day | wk | yr],
 Species Mass Concentration Source Rate {real},
 Units [$M/L^3 T$],

where unit of M is [kg | gm | lbm]; unit of T is [min | h | day | s | wk | yr]; and unit of L is [m | cm | mm | in | ft | yd].

7.17 Output Control Card

The Output Control card is used to specify reference nodes output and plotting output.

Format:

Line 0 “~Output Control”
 Line 1 N {integer} “line(s) of output control input to follow.”
 Line n Field Variable Output Time (for “output” and “plot” file) {real},
 Units [s | min | h | day | wk | yr],
 Next I-index of Reference Node 1 {integer},
 Line J-index of Reference Node 1 {integer},
 K-index of Reference Node 1 {integer},
 I-index of Reference Node 2 {integer},
 J-index of Reference Node 2 {integer},
 K-index of Reference Node 2 {integer},
 I-index of Reference Node 3 {integer},
 J-index of Reference Node 3 {integer},

K-index of Reference Node 3 {integer},
 I-index of Reference Node 4 {integer},
 J-index of Reference Node 4 {integer},
 K-index of Reference Node 4 {integer},
 Reference Node Output Frequency (Time Steps per Output) {integer},
 Next N {integer} “line(s) of output control input to follow.”
 Line
 Line n “plot” file field variable (see Table 4)
 Next N {integer} “line(s) of output control input to follow.”
 Line
 Line n reference node field variable (see Table 4)

Table 4. List of field variable available for “plot” file and reference node record.

<u>Field Variable Name in Input File</u>	<u>Name Used in Reference Node Record</u>
Liquid Pressure	P
Species Concentration	C
Liquid Saturation	SL
Liquid Phase Relative Permeability	KL
Liquid Density	DL
Total Hydraulic Head	HH
Volumetric Moisture	MC
X-Dir. Liquid Velocity	U
Y-Dir. Liquid Velocity	V
Z-Dir. Liquid Velocity	W
X-Dir. Species Velocity	UC
Y-Dir. Species Velocity	VC
Z-Dir. Species Velocity	WC
Tension Head	TH
Species Liq Concentration	CL
Species Sol Concentration	CS
Species Fix Concentration	CF
Species Fue Concentration	CP

8 References

1. Van Genuchten, M. Th., A closed-form equation for predicting the hydraulic conductivity of unsaturated soils. *Soil Sci. Soc. Am. J.*, 44(5), 892-898, 1980.
2. Brooks, R.H., and A.T. Corey, Hydraulic properties of porous media, *Hydrol. Pap. 3*, 27 pp., Colo. State Univ., Fort Collins, 1964.
3. Haverkamp, R., M. Vauclin, J. Touma, P. Wierenga, and G. Vachaud, A comparison of numerical simulation models for one-dimensional infiltration, *Soil Sci. America Journal*, 41, 285-294, 1977
4. Mualem, Y., A new model for predicting the hydraulic conductivity of unsaturated media. *Water Resour. Res.*, 12(3), 513-522, 1976.
5. Burdine, N.T., Relative permeability calculations from pore-size distribution data, *Am. Inst. Min. Eng. Pet. Trans.*, 198, 71-77, 1953.
6. Touma, J., and M. Vauclin, Experimental and numerical analysis of two-phase infiltration in a partially saturated soil, *Transport in Porous Media*, 27-55, 1986.
7. Konoplev A.V., Kopylova L.P., Bobovnikova Ts.I., Bulgakov A.A., and Siverina A.A. Distribution of ⁹⁰Sr and ¹³⁷Cs within the system of bottom sediments-water of the reservoirs in the areas adjacent to the Chernobyl NPP. *Meteorologiya and Hydrologiya*, 1, p. 35-42, 1992. (in Russian).
8. Millington, R.J., and J.P. Quirk, Permeability of porous solids. *Trans. Faraday Soc.*, 57, 1200-1207, 1961.
9. Frind E.O. Simulation of long-term transient density-dependent transport in groundwater, *Adv. Water Resour.*, 5, 73-86, 1982.
10. Philip, J.R., The theory of infiltration, 1, The infiltration equation and its solution, *Soil Sci.*, 83, 345-357, 1957.
11. El-Kadi, A.I., INFIL. International Groundwater Modeling Center, Holcomb Research Institute, Indiana, 1987.
12. Ross, B., J.W. Mercer, S.D. Thomas, and B.H. Lester, Benchmark Problems for Repository Siting Models. NUREG/CR-3097, U.S.Nuclear Regulatory Commission, Washington, D.C., 1982.
13. Philip, J.R., Numerical solution of equations of the diffusion type with diffusivity concentration-dependent, *Trans. Faraday Soc.*, 51, 885-892, 1955.
14. Smiles, D.E., J.R. Philip, J.H.Knight, and D.E. Elrick, Hydrodynamic dispersion during absorption of water by soil, *Soil Sciences America Journal*, 42, 229-234, 1977.
15. Chernobyl accident. Edited by V.G.Baryakhtar. Kiev, Naukova dumka, 1995.
16. Borovoi A.A, Evstratenko A.S., Krinitsyn A.P., Matyukhin A.P., Pavlyuchenko N.I., Simanoskaya I.Ya., Khorenko I.P. Shelter radioactive condition dynamics./ Shelter - 10 years. Main scientific research results. Chernobyl, Interdisciplinary Scientific and Technical Centre "Shelter", National Academy of Sciences of Ukraine, 1996, p. 100-111.

17. Pavlyuchenko N.I., Khorenko I.P. Review of works to study techno-geologic section and radionuclide contamination of groundwater for building area of the Shelter. // Problems of the Exclusion Zone, 1996, No 3, p. 58-65 (in Russian).
18. Selection and feasibility study of safety technology for removal of nuclear-hazard fission materials from rooms of accidentally destroyed unit-4 of the Chernobyl NPP on base of developed industrial technologies. Analysis and generalization of known data. Chernobyl-Kiev, State Company "Technocentre" for Treatment and Disposal of Mixed Hazardous Waste Report, No 01974006587, 1997.
19. On-going and Predictive Estimations of Radiogeologic Condition Changes of the Exclusion Zone. Development of Recommendations for Improvement of Groundwater Monitoring. Kiev, Institute of Geological Sciences Report, No 0195V022415, 1995.
20. White M.D., W.E.Nichols. MSTs: multiphase subsurface transport simulator. Theory manual. Richland, Washington, USA, Pacific Northwest Laboratory, PNL-8636, 1992.
21. White M.D., W.E.Nichols, MSTs: multiphase subsurface transport simulator. User's guide and reference. Richland, Washington, USA, Pacific Northwest Laboratory, PNL-8637, 1993.

Appendix

A. Input File of Philip's Infiltration Problem

```
~Simulation Title and Notes
Philip's Vertical Infiltration Problem
Sergey L. Kivva
IPMMS, Kiev
Monday, August 18, 1997
11:08:20 AM
0 line(s) of simulation title notes follows.
~Solution Schemes
false,false,false,
true,false,
2.,h,
.01,h,
1.001,
0.1,h,
true,
~Numerical Control
80,Maximum Residual,
1.0E-06,
Arithmetic Mean,Harmonic Mean,
~Grid Geometry
1,1,99,
1.,cm,1.,cm,15.,cm,0.,m,-15.,cm,
1 line(s) of grid geometry input follows.
Node 1,0.5,cm,
1 line(s) of grid geometry input follows.
Node 1,0.5,cm,
99 line(s) of grid geometry input follows.
Node 1, .15,cm,
Node 2, .30,cm,
Node 3, 0.45,cm,
Node 4, 0.60,cm,
Node 5, 0.75,cm,
Node 6, 0.90,cm,
Node 7, 1.05,cm,
Node 8, 1.20,cm,
Node 9, 1.35,cm,
Node 10, 1.50,cm,
Node 11, 1.65,cm,
Node 12, 1.80,cm,
Node 13, 1.95,cm,
Node 14, 2.10,cm,
Node 15, 2.25,cm,
Node 16, 2.40,cm,
```

Node 17, 2.55,cm,
Node 18, 2.70,cm,
Node 19, 2.85,cm,
Node 20, 3.00,cm,
Node 21, 3.15,cm,
Node 22, 3.30,cm,
Node 23, 3.45,cm,
Node 24, 3.60,cm,
Node 25, 3.75,cm,
Node 26, 3.90,cm,
Node 27, 4.05,cm,
Node 28, 4.20,cm,
Node 29, 4.35,cm,
Node 30, 4.50,cm,
Node 31, 4.65,cm,
Node 32, 4.80,cm,
Node 33, 4.95,cm,
Node 34, 5.10,cm,
Node 35, 5.25,cm,
Node 36, 5.40,cm,
Node 37, 5.55,cm,
Node 38, 5.70,cm,
Node 39, 5.85,cm,
Node 40, 6.00,cm,
Node 41, 6.15,cm,
Node 42, 6.30,cm,
Node 43, 6.45,cm,
Node 44, 6.60,cm,
Node 45, 6.75,cm,
Node 46, 6.90,cm,
Node 47, 7.05,cm,
Node 48, 7.20,cm,
Node 49, 7.35,cm,
Node 50, 7.50,cm,
Node 51, 7.65,cm,
Node 52, 7.80,cm,
Node 53, 7.95,cm,
Node 54, 8.10,cm,
Node 55, 8.25,cm,
Node 56, 8.40,cm,
Node 57, 8.55,cm,
Node 58, 8.70,cm,
Node 59, 8.85,cm,
Node 60, 9.00,cm,
Node 61, 9.15,cm,
Node 62, 9.30,cm,
Node 63, 9.45,cm,

Node 64, 9.60,cm,
Node 65, 9.75,cm,
Node 66, 9.90,cm,
Node 67, 10.05,cm,
Node 68, 10.20,cm,
Node 69, 10.35,cm,
Node 70, 10.50,cm,
Node 71, 10.65,cm,
Node 72, 10.80,cm,
Node 73, 10.95,cm,
Node 74, 11.10,cm,
Node 75, 11.25,cm,
Node 76, 11.40,cm,
Node 77, 11.55,cm,
Node 78, 11.70,cm,
Node 79, 11.85,cm,
Node 80, 12.00,cm,
Node 81, 12.15,cm,
Node 82, 12.30,cm,
Node 83, 12.45,cm,
Node 84, 12.60,cm,
Node 85, 12.75,cm,
Node 86, 12.90,cm,
Node 87, 13.05,cm,
Node 88, 13.20,cm,
Node 89, 13.35,cm,
Node 90, 13.50,cm,
Node 91, 13.65,cm,
Node 92, 13.80,cm,
Node 93, 13.95,cm,
Node 94, 14.10,cm,
Node 95, 14.25,cm,
Node 96, 14.40,cm,
Node 97, 14.55,cm,
Node 98, 14.70,cm,
Node 99, 14.85,cm,

~Inactive Nodes

0 line(s) of inactive nodes input follows.

~Rock or Soil Types

0 lines(s) of rock or soil types notes follows.

1 line(s) of rock or soil types input follows.

Clay,1,1,1,1,1,99,

~Mechanical Properties

1 line(s) of mechanical properties input follows.

Clay,0.495,0.371,0.371,,gm/cm^3,constant,,m,,m,

~Hydraulic Properties

1 line(s) of hydraulic properties input follows.

Clay,1.23e-7,1.23e-7,1.23e-7,hc:m/s,0.124,1/m,
~Species Properties
0 line(s) of species properties input follows.
~Soil Characteristics
1 line(s) of soil characteristics input to follow.
Clay,Haverkamp 2,739.0,cm,4.0,1.E+20,m,
~Liquid Relative Permeability Properties
1 line(s) of liquid relative permeability input to follow.
Clay,Haverkamp 2,124.6,1.77,1.E-20,,
~Liquid Boundary Conditions
2 line(s) of liquid boundary conditions input follows.
Z-Direction: Top Surface,Dirichlet @ Boundary,constant,101325.,Pa (absolute),1,1,1,1, 99,99,
Z-Direction: Bottom Surface,Dirichlet @ Boundary,constant,42387.6,Pa (absolute),1,1,1, 1,1,1,
~Species Boundary Conditions
0 line(s) of species boundary conditions input follows.
~Initial Conditions
1 line(s) of initial conditions input follows.
Liquid Pressure,42387.6015,Pa (absolute),0.0,1/m,0.0,1/m,0.0,1/m,1,1,1,1,1,99,
~Sources & Sinks
0 line(s) of sources & sinks input to follow.
~Output Control
1 line(s) of output control input follows.
2.0,h,
1,1,99,1,1,80,1,1,70,1,1,1,1,
7 line(s) of output control input follows.
Tension Head,
Liquid Pressure,
Liquid Saturation,
Liquid Phase Rel. Permeability,
Total Hydraulic Head,
Volumetric Moisture Content,
Z-Dir. Liquid Velocity,
5 line(s) of output control input follows.
Liquid Pressure,
Liquid Saturation,
Total Hydraulic Head,
Volumetric Moisture Content,
Z-Dir. Liquid Velocity,

B. Input File of Unsaturated Species Transport Problem

~Simulation Title and Notes
Species Unsaturated Transport Test
Sergey L. Kivva
IPMMS, Kiev
Monday, August 11, 1997
10:28:20 AM
0 line(s) of simulation title notes follows.

```
~Solution Schemes
false,false,false,
true,true,
9504.0,s,
1.0,s,
1.500,
150.0,s,
true,
~Numerical Control
80,Maximum Residual,
1.0E-06,
Harmonic Mean,Harmonic Mean,
~Grid Geometry
150,1,1,
20.,cm,1.,cm,1.,cm,0.,cm,0.,cm,
150 line(s) of grid geometry input follows.
Node 1, .02,cm,
Node 2, .06,cm,
Node 3, .10,cm,
Node 4, .14,cm,
Node 5, .18,cm,
Node 6, .22,cm,
Node 7, .26,cm,
Node 8, .30,cm,
Node 9, .34,cm,
Node 10, .38,cm,
Node 11, .42,cm,
Node 12, .46,cm,
Node 13, .50,cm,
Node 14, .54,cm,
Node 15, .58,cm,
Node 16, .62,cm,
Node 17, .66,cm,
Node 18, .70,cm,
Node 19, .74,cm,
Node 20, .78,cm,
Node 21, .82,cm,
Node 22, .86,cm,
Node 23, .90,cm,
Node 24, .94,cm,
Node 25, .98,cm,
Node 26, 1.02,cm,
Node 27, 1.06,cm,
Node 28, 1.10,cm,
Node 29, 1.14,cm,
Node 30, 1.18,cm,
Node 31, 1.22,cm,
```

Node 32, 1.26,cm,
Node 33, 1.30,cm,
Node 34, 1.34,cm,
Node 35, 1.38,cm,
Node 36, 1.42,cm,
Node 37, 1.46,cm,
Node 38, 1.50,cm,
Node 39, 1.54,cm,
Node 40, 1.58,cm,
Node 41, 1.62,cm,
Node 42, 1.66,cm,
Node 43, 1.70,cm,
Node 44, 1.74,cm,
Node 45, 1.78,cm,
Node 46, 1.82,cm,
Node 47, 1.86,cm,
Node 48, 1.90,cm,
Node 49, 1.94,cm,
Node 50, 1.98,cm,
Node 51, 2.02,cm,
Node 52, 2.06,cm,
Node 53, 2.10,cm,
Node 54, 2.14,cm,
Node 55, 2.18,cm,
Node 56, 2.22,cm,
Node 57, 2.26,cm,
Node 58, 2.30,cm,
Node 59, 2.34,cm,
Node 60, 2.38,cm,
Node 61, 2.42,cm,
Node 62, 2.46,cm,
Node 63, 2.50,cm,
Node 64, 2.54,cm,
Node 65, 2.58,cm,
Node 66, 2.62,cm,
Node 67, 2.66,cm,
Node 68, 2.70,cm,
Node 69, 2.74,cm,
Node 70, 2.78,cm,
Node 71, 2.82,cm,
Node 72, 2.86,cm,
Node 73, 2.90,cm,
Node 74, 2.94,cm,
Node 75, 2.98,cm,
Node 76, 3.02,cm,
Node 77, 3.06,cm,
Node 78, 3.10,cm,

Node 79, 3.14,cm,
Node 80, 3.18,cm,
Node 81, 3.22,cm,
Node 82, 3.26,cm,
Node 83, 3.30,cm,
Node 84, 3.34,cm,
Node 85, 3.38,cm,
Node 86, 3.42,cm,
Node 87, 3.46,cm,
Node 88, 3.50,cm,
Node 89, 3.54,cm,
Node 90, 3.58,cm,
Node 91, 3.62,cm,
Node 92, 3.66,cm,
Node 93, 3.70,cm,
Node 94, 3.74,cm,
Node 95, 3.78,cm,
Node 96, 3.82,cm,
Node 97, 3.86,cm,
Node 98, 3.90,cm,
Node 99, 3.94,cm,
Node 100, 3.98,cm,
Node 101, 4.02,cm,
Node 102, 4.06,cm,
Node 103, 4.10,cm,
Node 104, 4.14,cm,
Node 105, 4.18,cm,
Node 106, 4.22,cm,
Node 107, 4.26,cm,
Node 108, 4.30,cm,
Node 109, 4.34,cm,
Node 110, 4.38,cm,
Node 111, 4.42,cm,
Node 112, 4.46,cm,
Node 113, 4.50,cm,
Node 114, 4.60,cm,
Node 115, 4.70,cm,
Node 116, 4.80,cm,
Node 117, 4.90,cm,
Node 118, 5.00,cm,
Node 119, 5.10,cm,
Node 120, 5.20,cm,
Node 121, 5.30,cm,
Node 122, 5.40,cm,
Node 123, 5.50,cm,
Node 124, 5.60,cm,
Node 125, 5.70,cm,

Node 126, 5.80,cm,
 Node 127, 5.90,cm,
 Node 128, 6.00,cm,
 Node 129, 6.20,cm,
 Node 130, 6.40,cm,
 Node 131, 6.60,cm,
 Node 132, 6.80,cm,
 Node 133, 7.00,cm,
 Node 134, 7.20,cm,
 Node 135, 7.40,cm,
 Node 136, 7.60,cm,
 Node 137, 7.80,cm,
 Node 138, 8.00,cm,
 Node 139, 8.50,cm,
 Node 140, 9.50,cm,
 Node 141, 10.50,cm,
 Node 142, 11.50,cm,
 Node 143, 12.50,cm,
 Node 144, 13.50,cm,
 Node 145, 14.50,cm,
 Node 146, 15.50,cm,
 Node 147, 16.50,cm,
 Node 148, 17.50,cm,
 Node 149, 18.50,cm,
 Node 150, 19.50,cm,
 1 line(s) of grid geometry input follows.
 Node 1,0.5,cm,
 1 line(s) of grid geometry input follows.
 Node 1, 0.5,cm,
 ~Inactive Nodes
 0 line(s) of inactiveNodes input follows.
 ~Rock or Soil Types
 0 line(s) of rock or soil types notes follows.
 1 line(s) of rock or soil types input follows.
 Sand,1,150,1,1,1,1,
 ~Mechanical Properties
 1 line(s) of mechanical properties input follows.
 Sand,0.45,0.45,0.30,,gm/cm^3,constant,1.0,,m,,m,
 ~Hydraulic Properties
 1 line(s) of hydraulic properties input follows.
 Sand,1.0,1.0,1.0,hc:cm/day,0.0,1/m,
 ~Species Properties
 1 line(s) of species properties input follows.
 Sand,Solute,1.1574074E-9,m^2/s,0.0,gm liq./gm sol.,,s,,,,,
 ~Soil Characteristics
 1 line(s) of soil characteristics input to follow.
 Sand,Tabular,Table No. 1,

2 line(s) of capillary tables input follows.
 1.0,.333333,m,
 0.0,1.0,m,
 ~Liquid Relative Permeability Properties
 1 line(s) of liquid relative permeability input to follow.
 Sand,Tabular vs Liquid Saturation,Table No. 1,
 2 line(s) of liquid permeability tables input follows.
 0.33333,0.0,
 1.0,1.0,
 ~Liquid Boundary Conditions
 1 line(s) of liquid boundary conditions input follows.
 X-Direction: West Surface,Dirichlet @ Boundary,constant,101325.,Pa (absolute),1,1,1,1,1,1,
 ~Species Boundary Conditions
 2 line(s) of species boundary conditions input follows.
 X-Direction: West Surface,Dirichlet @ Boundary,constant,1.0,1/liter,1,1,1,1,1,1,
 X-Direction: East Surface,Dirichlet @ Boundary,constant,0.1,1/liter,150,150,1,1,1,1,
 ~Initial Conditions
 2 line(s) of initial conditions input follows.
 Liquid Pressure,93157.21,Pa (absolute),0.0,1/m,0.0,1/m,0.0,1/m,1,150,1,1,1,1,
 Species Liquid Concentration,0.1,1/liter,0.0,1/m,0.0,1/m,0.0,1/m,1,150,1,1,1,1,
 ~Sources & Sinks
 0 line(s) of sources & sinks input to follow.
 ~Output Control
 3 line(s) of output control input follows.
 0.01,day,
 0.06,day,
 0.11,day,
 5,1,1,10,1,1,15,1,1,20,1,1,1,
 2 line(s) of output control input follows.
 Species Liq Concentration,
 Volumetric Moisture Content,
 4 line(s) of output control input follows.
 Liquid Pressure,
 Species Concentration,
 Volumetric Moisture Content,
 X-Dir. Liquid Velocity,

Document History

Document Title: SUSTOX - A Numerical Simulator for Fluid and Species
Transport in the Subsurface
RODOS number: RODOS(WG4)-??(??)-??
Version and status: Version 1.0 (draft)
Authors/Editors: S.L.Kivva
Address: IPMMS, pr.Glushkova, 42, 252207 Kiev, Ukraine
Issued by:
History:
Date of Issue: December 5, 1997
Circulation:
File Name: Report97.docDokument1
Date of print: September 20, 2000